Available online at www.sciencedirect.com
SCIENCE DIRECT®
ELSEVIER
Deep-Sea Research I 51 (2004) 849–864
DEEP-SEA RESEARCH PART I
www.elsevier.com/locate/dsr

Growth, reproduction and possible recruitment variability in the abyssal brittle star *Ophiocten hastatum* (Ophiuroidea: Echinodermata) in the NE Atlantic

John D. Gage[a,*], Roslyn M. Anderson[a], Paul A. Tyler[b], Rachel Chapman[b], Emily Dolan[b]

[a] *Dunstaffnage Marine Laboratory, Scottish Association for Marine Science, P.O. Box 3, Oban, Argyll PA37 1QA, Scotland, UK*
[b] *School of Ocean and Earth Sciences, University of Southampton, Southampton Oceanography Centre, Southampton SO14 3ZH, UK*

Received 14 January 2003; received in revised form 16 July 2003; accepted 20 January 2004

Abstract

Growth was studied from skeletal growth markers in the cosmopolitan abyssal brittle star *Ophiocten hastatm*. Samples for analysis were taken at five sites located in the southern (2900 m) and central (2000 m) Rockall Trough, at ca. 3000 and 4000 m in the Porcupine Seabight, and at 4850 m on the Porcupine Abyssal Plain. Growth bands were assumed to reflect an annual cycle in skeletal growth. Band measurements on arm vertebrae, standardised to disc diameter, were used to provide size-at-age data and size-increment data that took into account overgrowth of early bands in older individuals. The Richards growth function marginally provides best fit to pooled size-at-age data, although the asymptote-less Tanaka function and the Gompertz growth function also provided good fit to size-at-age data which showed a rather linear growth pattern with little indication of a growth asymptote. $\mathrm{Log_e}$ transformed size-increment data were linearised by applying the Ford–Walford method to approximate Gompertz growth so that growth could be compared at the five sites. Grouped linear regression and analysis of covariance showed no significant differences between growth at the sites and a common fitted regression. However, pairwise comparisons suggest growth differences with increasing bathymetric separation. Oocyte size frequencies measured from histological preparations of the gonad of specimens from the Porcupine Abyssal Plain indicate marked reproductive periodicity, with spawn-out in late winter that is likely followed by planktotrophic early development in spring with benthic settlement in summer. Although usually rare in the trawl and epibenthic sled samples, several years of successful recruitment followed by a period when recruitment was low or absent might explain size structure observed in a single unusually large sample from the Rockall Trough. This is consistent with previous observations during the late 1990s of a large population increase on the Porcupine Abyssal Plain. Analysis of growth bands of these specimens sampled in 1997 suggest the population increase derives from a single or small number of year classes recruited during the early 1990s.

Keywords: Ophiuroidea; Population dynamics; Growth comparison; Reproduction; Recruitment; Benthic environment; NE Atlantic; Rockall trough; Porcupine Seabight Porcupine Abyssal Plain

*Corresponding author. Tel.: +44-01631-562244; fax: +44-01631-565518.
E-mail address: jdg@sams.ac.uk (J.D. Gage).

0967-0637/$ - see front matter © 2004 Elsevier Ltd. All rights reserved.
doi:10.1016/j.dsr.2004.01.007

1. Introduction

Brittle stars are often quantitatively important elements of the benthic community in the deep ocean. Yet the population biology of deep-sea species, particularly those with an abyssal distribution, is poorly understood. *Ophiocten hastatum* Lyman 1878 (superseded synonym *O. latens* Koehler 1906, see Paterson et al., 1982) has an apparently cosmopolitan distribution typical of abyssal ophiuroids (Paterson, 1985). In the NE Atlantic *O. hastatum* is known from the Rockall Trough from 2000 to 2980 m (Gage et al., 1983; Harvey et al., 1988) to the Azores at depths of 1970–4700 m (Paterson, 1985). The brittle star is typically found in small numbers in bottom trawlings. Nothing is known of its population structure, growth and reproduction, although recent work indicates the brittle star, like its bathyal congener *O. gracilis* (Pearson and Gage, 1984), feeds selectively on phytodetritus (Bett et al., 2001; Iken et al., 2001).

We here provide (1) data on population abundance and size structure, (2) analyses of individual somatic growth from measurements of natural skeletal growth markers present in the vertebral ossicles of the arm from samples from five sites, and (3) data on reproductive biology from histological analysis of oocytes in gonads of individuals from samples taken at different times of the year. This new information is used to provide an interpretation of life history strategy of *O. hastatum*. Recruitment variability may help to explain how spatial and temporal variability in disc size frequencies of *O. hastatum* observed in samples at the different sites in the northeastern Atlantic might have occurred.

2. Material and methods

2.1. Samples

Samples came from five areas in the NE Atlantic (Fig. 1): (1) the SAMS Permanent Station, a repeat station in the southern Rockall Trough centred on 54°40′N, 12°16′W that was sampled from 1975 to 1992 by the Scottish Association for Marine Science, SAMS (previously Scottish Marine Biological Association, SMBA); (2) the Feni Ridge in the central Rockall Trough where a single sample had been taken by SAMS from 2000 m depth; (3) the Porcupine Seabight at ca. 3000 m, and (4) the Porcupine Seabight at ca. 4000 m, both sampled by the Southampton Oceanography Centre (SOC) in 1979 and 1980; (5) the Porcupine Abyssal Plain (centred on 48°50′N 16°30′W, ca. 4845 m depth) also sampled by SOC from 1978 up to 1998 and adopted for study by the E.U. *BENGAL* programme (1996–1999) and here referred to as the *BENGAL* station. Samples obtained from the *BENGAL* station by Institut Français de Recherche pour l'Exploitation de la Mer (IFREMER) is also used.

Samples from the SAMS Permanent Station were taken mainly using the Woods Hole pattern epibenthic sled (main bag mesh 1 mm, cod-end mesh 0.5 mm) that would be expected to retain all post-larval sizes of brittle stars entering the gear. Other samples from the SAMS Permanent Station were taken using a 3-m wide Agassiz trawl (cod-end mesh 10 mm) and a Semi-Balloon Otter Trawl (OTSB 14), with 13 mm stretch mesh at the cod end, both of which would not be expected to retain the smallest sizes of *O. hastatum*. The samples from the Porcupine Seabight were obtained using a larger version of the epibenthic sled with a 4.5 mm mesh main bag and 1 mm mesh cod end and referred to here as the SOC sled, while those from the *BENGAL* station were obtained using either the SOC sled, an OTSB 14 or the USNEL box corer which quantitatively samples 0.25 m^2 of seabed, with the sediment washed through a 0.25 mm sieve. Both this and the SOC sled hauls would be expected to retain post-larval brittle stars. Positional coordinates, depths and dates of these samples are listed in Table 1.

2.2. Population density and size structure

A large enough sample to plot disc-size frequencies for analysis of population size structure was available from only one sample, an Agassiz trawl haul from the SAMS Permanent Station in the southern Rockall Trough (sample AT121 taken in 1976). This had 145 individuals

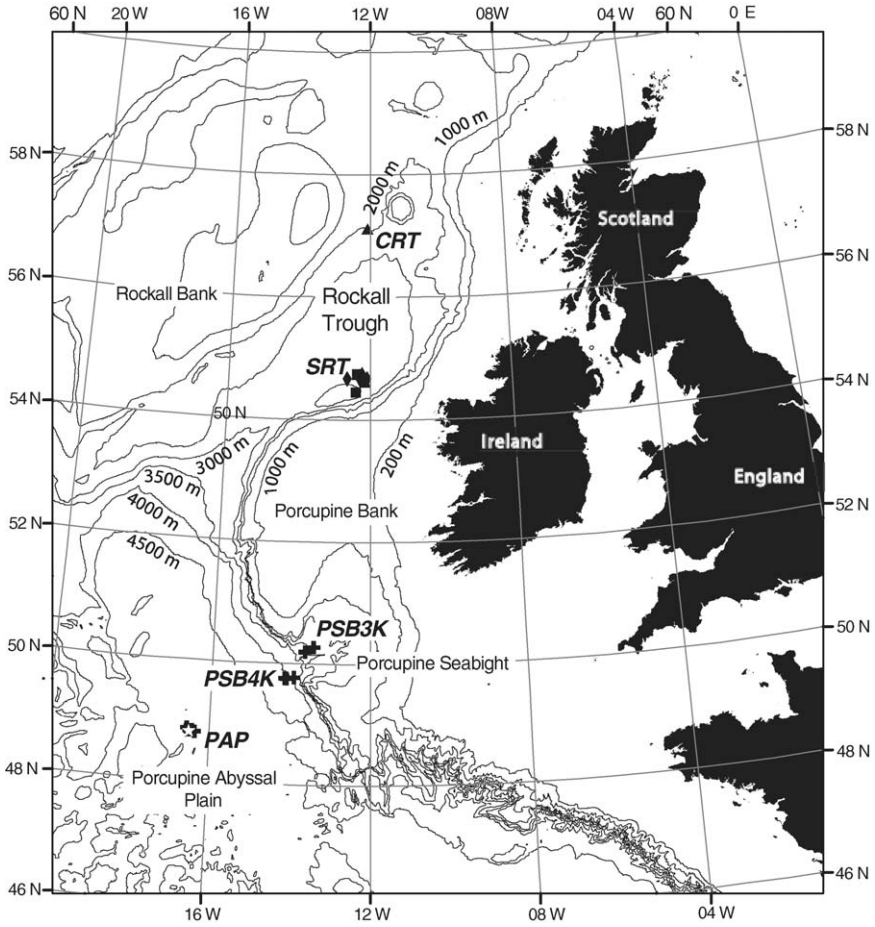

Fig. 1. Chart of study area in the NE Atlantic showing sample areas identified in Table 1. SRT, southern Rockall Tough, SAMS Permanent Sta; CRT, central Rockall Trough, Feni Ridge; PSB3K, ca. 3000 m, Porcupine Seabight; PSB4K, ca. 4000 m Porcupine Seabight; PAP, Porcupine Abyssal Plain, *BENGAL* sta. The symbols show positions of individual samples and the symbol relates to the sort of gear used: filled squares, WHOI epibenthic sled; filled crosses, SOC epibenthic sled; filled triangles, Agassiz trawl hauls; while the white star denotes the site of the box core samples from the *BENGAL* station (Porcupine Abyssal Plain). Bathymetry below the 200-m line is contoured at 1000 m intervals.

available for measurement from a total sample of 187. Disc-size frequencies are also plotted from aggregated OTSB, SOC sled and USNEL box corer samples from the *BENGAL* station on the Porcupine Abyssal Plain (all taken on various dates in 1996, 1997 and 1998). Disc diameter was measured on the alcohol-preserved specimens after blotting. Measurements were taken across the disc edge above the base of an arm (in this species overlying the arm insertion) across to the opposite inter-radius.

2.3. Ossicle growth banding

Specimens selected for study of ossicle growth banding always included the largest available, but as subsamples were not necessarily representative of population size structure. A section of arm was taken from near the arm insertion under the disc edge of the brittle star in order to study natural growth banding. We used the proximal-most part of the arm in order to minimise error in ageing a specimen whose arm might have regenerated. The

Table 1
Positions and depths for the different samples used in the present study arranged by area

Station	Depth (m)	Date	Latitude (N)	Longitude (W)
SAMS Permanent Station, southern RockallTrough				
ES 111	ca 2886	22/10/76	54°40′	12°16′
AT 121	2910	29/01/76	54°37′	12°09′
ES 143	ca 2892	14/04/78	54°41′	12°14′
ES 185	2907	10/04/81	54°44′	12°15′
9/82/5130	2925	30/04/81	54°45′	12°23′
(OTSB 14)				
ES 283	2946	15/04/85	54°39′	12°15′
3/85/5	22870–2980	15/04/85	54°27	12°25′
(OTSB 14)				
AT 351	2898	20/10/87	54°40′	12°12′
ES 352	2880	20/10/87	54°42′	12°19′
ES 395	2900	02/07/90	54°39′	12°18′
ES 401	2900	10/09/90	54°40′	12°16′
ES 411		16/12/90	54°40′	12°06′
ES 421	2900	17/11/91	54°40′	12°16′
Central Rockall Trough (Feni Ridge)				
AT 107	ca 2,000	11/07/76	57° 07′	12° 06′
ca. 3000 m Porcupine Seabight				
9756#14	3080–3097	15/04/78	50°04.0′	13°55.6′
(SOC sled)			50°04.3′	13° 53.2′
10113#1	2755–2760	10/09/79	50°16.1′	13°31.6′
(SOC sled)			50°16.3′	13°32.3′
10114#1	2129–2147	10/09/79	49°45.6′	14°08.2′
(SOC sled)			49°45.0′	14°08.0′
50913#1	3000–3040	12/11/80	50°11.9′	13°39.8′
(SOC sled)			50°11.3′	13°41.3′
ca. 4000 m, Porcupine Seabight				
10115#1	3900–3950	11/09/79	49°45.4′	14°10.3′
(SOC sled)				
50812#1	4080–4100	03/08/80	49°46.3′	13°56.0′
(SOC sled)			49°45.6′	13°56.6′
BENGAL station, Porcupine Abyssal Plain				
12930#39	4840	07/09/96	48°49.95′	16°29.40′
(BC)				
12930#63	4840	13/03/97	48°49.92′	16°29.76′
(BC)				
13077#23	4844	18/03/97	48°49.28′	16°30.56′
(BC)				
13078#29[a]	4844–4847	04/04/97	48°56.20′	16° 22.77′
(OTSB 14)			48° 47.35′	16° 33.23′
13200#20	4844	08/07/97	48°49.80′	16°29.62′
(BC)				
13200#35[a]	4842–4845	11/07/97	48°44.03′	16° 32.82′
(OTSB 14)			48°55.85′	16°40.22′
13200#47	4844	14/07/97	48°49.39′	16°30.27′
(BC)				
13200#60[a]	4843–4847	17/07/97	48°52.11′	16°26.66′

Table 1 (*continued*)

Station	Depth (m)	Date	Latitude (N)	Longitude (W)
(OTSB 14)			48°48.34′	16°42.01′
13200#88[a]	4852–4845	23/07/97	48°52.10′	16°25.47′
(SOC sled)			48°48.52′	16°36.01
54301#8[a]	4839–4844	22/10/97	48°49.1′	16°38.4′
(OTSB 14)			48°50.5′	16°27.0′
13368#51[a]	4840–4840	18/03/98	48°49.71′	16°28.42′
(OTSB 14)			48°48.88′	16°20.61′
13627#10[a]	4835–4837	30/09/98	48°53.06′	16°42.06′
(OTSB 14)			48°58.09′	16°45.02′
13627#17	4837	03/10/98	48°49.90′	16°30.50′
(BC)				
13627#23[a]	4837–4874	05/10/98	48°58.93′	16°45.22′
(OTSB 14)			49°03.88′	16°40.66′

Except where indicated by the prefix ES or AT, gear type is indicated by gear abbreviation in parentheses: ES denotes WHOI pattern epibenthic sled; AT'Agassiz trawl; OTSB 14, otter trawl; SOC sled, Southampton Oceanography Centre pattern epibenthic sled; and BC, USNEL 0.25 m^2 box corer.

[a] Indicates samples used for reproductive studies.

arm segment was prepared for examination of the vertebral ossicles according to the procedure of Gage (1990a, b). The vertebral ossicles, with the proximal two pairs of the wing-like fossae (which provide intervertebral muscle insertions) uppermost (Fig. 2A), were mounted on stubs, sputter-coated with gold in vacuum, and examined using a Jeol JSM-35C scanning electron microscope (SEM). Digital photographs were assembled for each image directly from the SEM's raster scan, normally used for film photography, using custom software. Growth bands were measured as radii as described by Dahm (1993) and Gage (2003) directly from SEM photographs, usually along two or more radial axes.

2.4. Growth analysis

The growth band measurements were treated as size-at-age data and size-increment data. For size-at-age, ossicle sizes and putative age pairs were assembled for all growth-band radius measurements. Following the approach described by Brey et al. (1995), the general growth model of Schnute (1981):

$$S_t = \left[y_1^B + (y_2^B - y_1^B)\frac{1 - e^{[-A*(t-\tau_1)]}}{1 - e^{[-A*(\tau_2-\tau_1)]}} \right]^{1/B},$$

which has four parameters, two constants A (time $^{-1}$) and B (dimensionless) and the sizes y_1 and y_2, was applied to establish a suitable growth function for size-at-age, S_t. The two age values τ_1 and τ_2 are user-chosen and correspond to the youngest and oldest individuals in the sample, respectively, and the starting values y_1 and y_2 set accordingly. Special cases of Schnute's general growth model resemble historical growth models, such as the decaying exponential type von Bertalanffy growth function:

$$S_t = S_\infty \left(1 - e_0^{-K(t-t_0)}\right),$$

where S_∞ is the asymptotic size, K the rate of approach to this asymptote and t_0 the age at which disc diameter would be zero, and sigmoidal type models such as the Gompertz growth function

$$S_t = S_\infty e^{-e^{[-K(t-t^*)]}}$$

and Richards growth function

$$S_t = S_\infty * \left(1 + 1/D\, e^{-K(t-t^*)}\right)^{-D},$$

where parameter t^* is the time of growth inflexion, and D (Richards function only) influences the shape of the curve. Schnute (1981) should be consulted for full explanation and mathematical derivation of these historical models in relation to Schnute's generalised growth model.

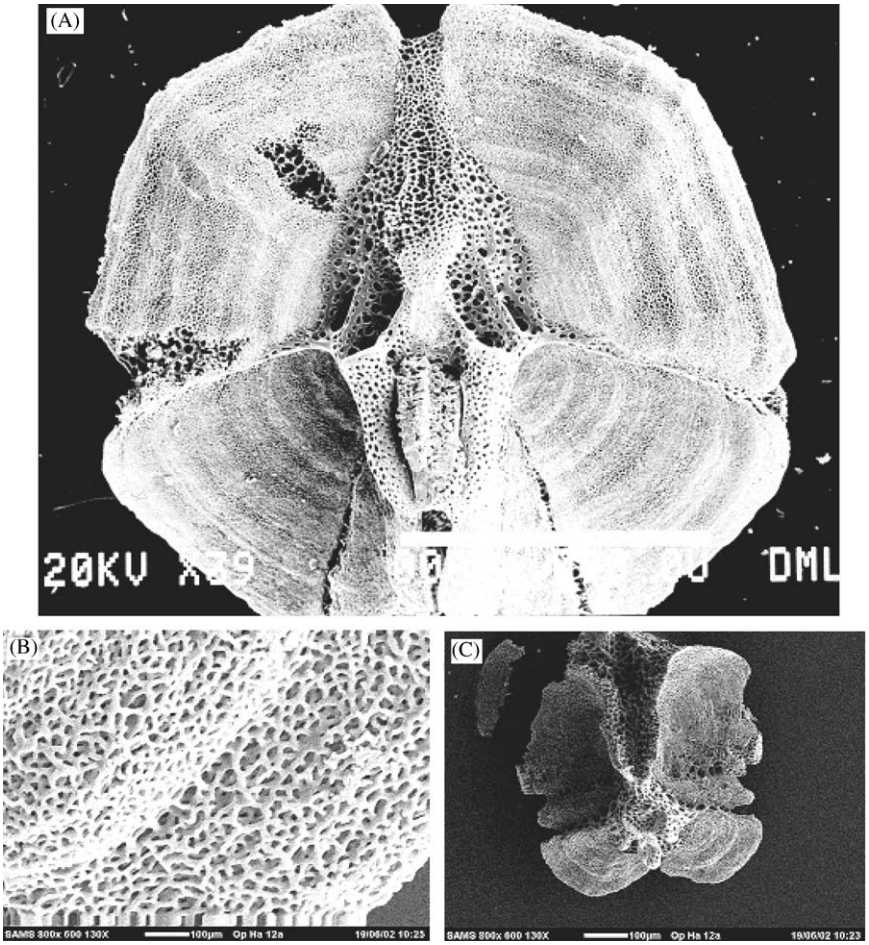

Fig. 2. SEM photographs of growth banding on the face of the intervertebral muscle-attachment fossae on the proximal face of arm ossicles taken from near the disc edge of *O. hastatum*. (A) Whole face of ossicle from a specimen (13.9 mm DD) from sample ES283 from the SAMS Permanent Station at ca. 2900 m in the southern Rockall Trough. (B) Close-up view of a pair of lower fossae of a specimen (6.5 mm *DD*) from the *BENGAL* station on the Porcupine Abyssal Plain (Station 13200#88). This shows how the growth-banding pattern is formed from successive zones of fine-pored stereom (reflecting slow growth) and coarse-pored, more open stereom (reflecting rapid growth). (C) Wider area view of one of the fossae in B showing the pattern in surface relief where the outer edge of fine-pored stereom forms the crest of a wave, the edge of which was used to provide a marker for the growth-band measurements taken from the centre of the ossicle.

Because of the rather linear pattern spacing typically seen in the growth zones of *O. hastatum* (see Fig. 2A) we also applied the Tanaka growth function (Tanaka, 1982):

$$S_t = 1/(f^{0.5}) * \ln(2 * f * (t - c) + 2 * [f^2 * (t - c)^2 + f * a]^{0.5}) + d$$

to the data. The four parameters of the Tanaka growth function determine the shape of the growth curve (which does not have an asymptote); a is related to maximum growth rate approximately $1/a^{0.5}$, c is the age at which growth rate is maximal, d determines body size at which growth rate is maximal, and of the rate of change in the growth rate. Ebert et al. (1999) provides lucid explanation of how these parameters determine a growth curve that incorporates early lag and exponential growth phases often observed in marine invertebrates (Yamaguchi, 1975).

Growth parameters were fitted, using the Microsoft Excel computation worksheet of Brey (2001), by means of iterative non-linear regression using Excel's SOLVER routine.

For size increment data each data pair consists of ossicle (diameter) size S_t at time t and a subsequent measurement of size S_{t+x} at time $t+x$ of an individual. In the present case because the band spacing is presumed to be annual, $x = 1$ yr. The size increment data pairs were $\log_e$ transformed in order to approximate growth according to the Gompertz growth function (Brey, 2001) when plotted as disc diameter data pairs of size at time t and size at time $t+1$ yr by the Ford–Walford method (Crisp, 1984). This provides a data linearisation allowing easier comparison of growth at the five sites. Comparison was made by grouped linear regression with covariance analysis (Armitage and Berry, 1994; Zar, 1998) to compare the slopes and levels (intercepts) of linear regressions fitted to the size-increment pairs for each of the five sites.

2.5. Analysis of gametogenic biology

Specimens used for study of reproductive histology were each measured as disc diameter and the disc then decalcified in RDC rapid decalcifying agent (CellPath, plc, Newtown, Wales, UK). After ~30 min the disc was transferred to 70% propan-2-ol overnight. Up to five specimens were available from each trawl haul taken at the *BENGAL* station on the Porcupine Abyssal Plain on eight different dates from 29 April 1997 to 5 October 1998. Individual discs were dehydrated, cleared and embedded in paraffin wax. Sections of the whole disc were cut at 7 μm and stained with Mayer's haemalum and counterstained with eosin. Sections were examined under compound microscope and the sections digitally frame grabbed. Images of oocytes where the section had passed through the cell nucleus were analysed using image analysis software by outlining the oocyte and calculating ferret diameter (diameter if the oocyte was a sphere). This is necessary, particularly for the well-developed ovary, because the packed, ripe oocyte typically has an irregular outline. These data were used to construct oocyte size/frequency data for each month along with the mean and standard deviation of oocytes in each oocyte size cohort.

3. Results

3.1. Assumptions of growth analysis

We assumed the growth bands reflect an annual cycle in skeletal growth. The grounds for this assumption are summarised in the Discussion. The end of winter growth is interpreted as a band of fine-pored stereom (also recognisable as an often abruptly ending, wave-like ridge in the surface relief) separating it from the beginning of new growth that was recognisable as coarse-pored stereom. This provides a less ambiguous marker than the midpoint of the fine-pored, winter growth zone, and was therefore used to separate annual growth bands (Figs. 2A and B). Because the marks were also often clearly expressed on the lower pair of fossae (Fig. 2C) measurements were made on these as well. Even if not utilised the banding expressed on all fossa surfaces was used to decide where to measure the bands. This was because on some fossae the line might not be clear all the way along its length.

The measured radius of each growth band (taken from a line along the midpoint of the ossicle) was later standardised to the disc diameter of the ophiuroid as a proportion of the full radius of the fossa in relation to the measured disc diameter. This interpolation of previous disc sizes measured from the inner growth bands assumes that the previous growth in size of the arm ossicles linearly tracks that of the disc (Gage, 1990a). The assumption was checked from measurements of arm width across the most proximal part of the arm (the part near its attachment under the outer edge of the disc used in studying growth bands) in relation to disc diameter. A power curve relationship of arm width on disc diameter provided only a slightly better fit than the linear relationship (Fig. 3) and the closeness of the two lines fitted to individuals over the wide range in size plotted in Fig. 3 suggests a linear relationship

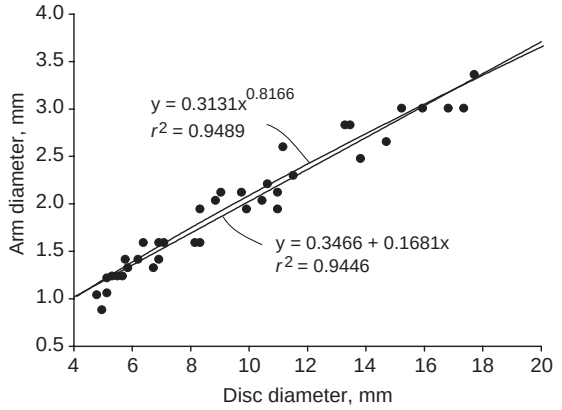

Fig. 3. Width of the arm (measured near its insertion to the disc) plotted on disc diameter with fitted linear and power curve regressions.

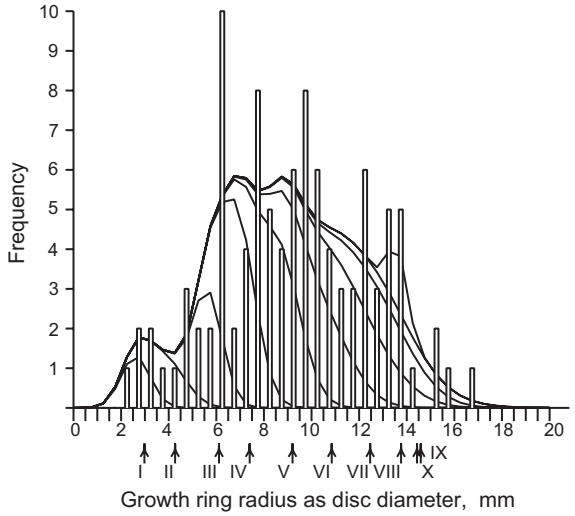

Fig. 4. Frequencies in measurements of ossicle growth band radius standardised to disc diameter (narrow open bars) showing a fitted normal mixture for a very large or infinite population plotted with very fine size intervals based the means, SD and relative numbers for each interpreted age class in these measurements, with the constituent components corresponding to each age class shown separated (labelled in roman numerals). The position of the means along the size axis is indicated by arrows.

provides reasonable fit to all except the most early growth phase.

3.2. Error in 'reading' arm ossicle age by overgrowth of early bands

Possible error in reading age on the ossicles of large specimens of *O. gracilis* was found to result from overgrowth of the first, and perhaps the second, growth band as a consequence of outward development of the massive articular stereom from the central part of the ossicle (Gage, 2003). This was first noticed in the inshore species *O. ophiura* and *O. affinis* (Dahm, 1993). With *O. hastatum* overgrowth might lead to error in the assignment of age to growth marks necessary in order to provide back-calculated size-at-age data necessary to fit a growth model. A strategy similar to that applied to *O. gracilis* by Gage (2003) was used to correct age of bands 'read' from large-sized specimens by comparing these data with those from the smallest specimens. With *O. gracilis* it was possible to check on this from age structure interpreted from peaks in disc-size frequencies. This was not possible with *O. hastatum* because no sufficiently large sample from a fine-meshed sampler was available. Instead the pooled frequencies of the growth band measurements were examined in order to see whether there was any pattern of peaks and troughs corresponding to the approximate size limits for each band (Fig. 4), as described by Dahm and Brey (1998). The, mainly single-frequency, peaks in the pooled growth bands seem poorly correlated to the means of the interpreted component age classes (Table 2). Fig. 4

Table 2
Back-calculated disc diameters and size-at-age read from growth bands in vertebral ossicles in the arm from specimens from SAMS Permanent Station in the southern Rockall Trough, giving the mean, and its standard deviation (SD) for the disc diameter (DD) size at each putative age

Age	*N*	Mean DD (mm)	SD (mm)
1	3	2.65	0.50
2	4	3.61	0.60
3	9	5.61	0.76
4	19	7.02	0.80
5	19	8.71	1.03
6	16	10.42	1.27
7	15	11.96	1.58
8	9	13.21	1.46
9	4	14.01	1.90
10	3	13.85	0.35

also shows a fitted a normal-distribution mixture based on these means, along with standard deviation and relative proportions (based on numbers in each interpreted age class), using a procedure described in Gage (2003). The considerable degree of overlapping in these components makes clear these frequencies are unlikely to inform interpretation of underlying age structure.

Assignment of age to the individual bands therefore had to employ the somewhat arbitrary process where the degree of overgrowth, and hence the age corresponding to the first visible band, was influenced by the size of the brittle star relative to a growth curve fitted to individuals $< \sim 7$ mm disc diameter. By analogy with its congener *O. gracilis* (where early growth could be tracked in time series of size frequency distributions), these animals were judged to be small enough not to have had the first growth band on the fossae overgrown by the massive central articular stereom. This, however, makes the assumption that the two species have similar patterns in skeletal arm growth. This seems reasonable from the similarity in morphology and growth band pattern of the arm ossicles (cf. Fig. 1 with Fig. 2 in Gage, 2003). A Schnute growth curve (see below) generated for a subset of the remaining specimens (>7 mm, <10 mm disc diameter), where the first band was arbitrarily set at 1, was moved right along the age axis until the best match with that for the small individuals was obtained. The age of the first band was then adjusted accordingly. If there were specimens $> \sim 10$ mm disc diameter the procedure was repeated. This was because of the possibility that later bands might also be overgrown.

3.3. Population density and size structure

Size frequencies of disc diameter measured from the single large sample taken in 1976 (AT121) from the SAMS Permanent Station in the southern Rockall Trough are given in Fig. 5A. Frequencies from the aggregated samples from the *BENGAL* station on the Porcupine Abyssal Plain are shown in Fig. 5B). It should be remembered these came from samples taken over 3 yr (1996–1998) and hence should not be compared directly with that from AT121.

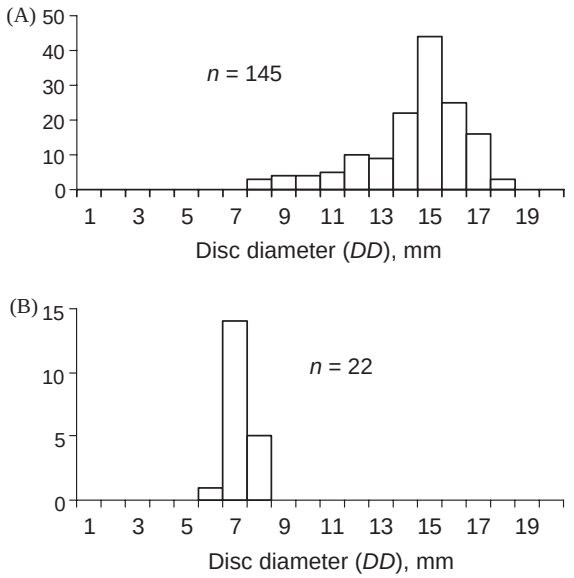

Fig. 5. Disc size frequencies of samples of *O. hastatum* (A), from sample AT121 from Rockall Trough permanent station; (B) from specimens from aggregated samples from the *BENGAL* station on the Porcupine Abyssal Plain. *n* is the number of individuals in the sample (AT121) or aggregated samples (*BENGAL* station) examined.

The maximum disc size among these individuals measured (17.7 mm) well exceeded the known maximum disc diameter for this species of 12 mm (Paterson et al., 1982).

3.4. Growth of O. hastatum from size-at-age data

Size-at-age data, expressed as disc diameter was collected from measurements of natural growth lines on the vertebral ossicles of 23 individuals (yielding 101 size increment pairs) out of 29 specimens of *O. hastatum* from the SAMS Permanent Station in the southern Rockall Trough, 7 (22 size increment pairs) from 11 specimens from the Feni Ridge in the central Rockall Trough, 4 (17 size increment pairs) out of 8 specimens from around 3000 m in the Porcupine Seabight, 4 (11 size increment pairs) out 9 specimens from around 4000 m in the Porcupine Seabight and 10 (31 size increment pairs) out of 15 examined from the *BENGAL* station on the Porcupine Abyssal Plain. Schnute's general growth model was fitted to the pooled 182 pairs of disc

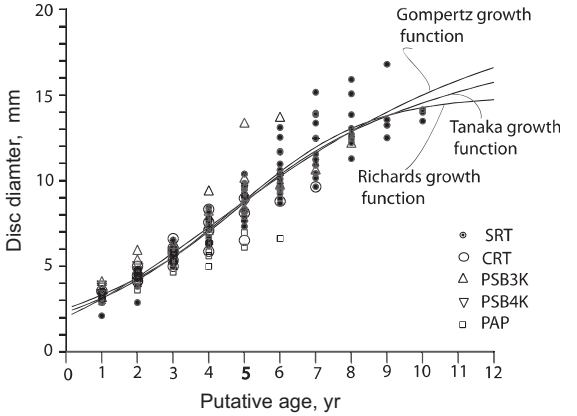

Fig. 6. Disc size-at-age (DD_t) measurements read from growth bands of *O. hastatum* with fitted Richards, Tanaka and Gompertz growth curves fitted to the pooled data, where: $DD_t = 14.86*(1 + 1/0.425\,e^{-0.632(t-5.117)})^{-0.425}$ (Richards function), $DD_t = 1/(0.324^{0.5})\ln(2 \times 0.324*(t - 4.497) + 2[0.057^2(t-4.497)^2 + 0.057 \times 0.324]^{0.5}) + 13.511$ (Tanaka function), $DD_t = 20.350\,e^{-e^{[-0.202(t-4.167)]}}$ (Gompertz function). Size at age points from the five sites are identified by a different symbol: SAMS Permanent Sta, southern Rockall Trough, filled circles; Feni Ridge, central Rockall Trough, open circles, ca. 3000 m Porcupine Seabight, triangles; ca. 4000 m Porcupine Seabight, inverted triangles; *BENGAL* Sta, Porcupine Abyssal Plain, open squares.

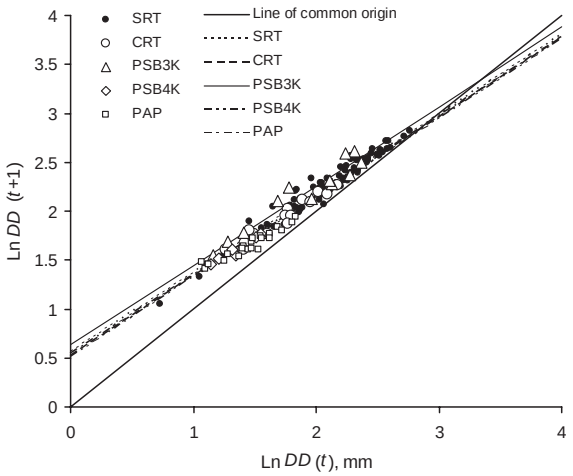

Fig. 7. Log_e-transformed disc diameter size-increment pairs plotted by the Ford–Walford method showing linear regression lines fitted to the data for each site and the intersections of these with the y-axis (intercept) and the line of common origin. Size-increment points from each of the five sites identified by symbol: SAMS Permanent Sta, southern Rockall Trough, filled circles; Feni Ridge, central Rockall Trough, open circles; ca. 3000 m Porcupine Seabight, open triangles; ca. 4000 m Porcupine Seabight, open diamonds; *BENGAL* Sta, Porcupine Abyssal Plain, open squares.

diameter-at-age data. The resulting common growth curve (Fig. 6) corresponds to the four-parameter Richards growth model.

Fit of these pooled size increment pairs to the asymptote-less Tanaka model provides only marginally inferior fit (residual sum of squares, RRS = 227.31, $r^2 = 0.88$) compared to the Richards function (RRS = 226.09, $r^2 = 0.89$) and only slightly better than the Gompertz growth function (RRS = 232.50, $r^2 = 0.88$). The Richards, Tanaka and Gompertz growth curves, along with parameter values, fitted to the pooled size-at-ages from the five sites are given in Fig. 6.

The log_e-transformed size-increment pairs are plotted with fitted linear regression lines for each site in Fig. 7. Grouped linear regression with covariance analysis compared regression parameters for the sites in relation to a common fitted function. This shows that a common slope is significant and that the differences between this and the slopes for each site are not significant. However, pairwise comparison for slopes and intercepts indicates (Table 3) some significant growth differences ($P < 0.05$) between sites with the greatest bathymetric separation.

3.5. Gametogenic periodicity

The gametogenic pattern shows evidence of strongly seasonal (annual) periodicity (Fig. 8); oogonia and young oocytes being found in the March and April samples. The summer samples showed between-sample variation in oocyte development, while the early autumn samples show a wide range of oocyte sizes up to a maximum of 140 μm diameter. No winter samples are available to determine the later stages of gametogenesis.

4. Discussion

4.1. Growth bands as annual growth markers

An assumption of a seasonal growth pattern causing the growth-banding pattern visible on the

Table 3
Results from grouped linear regression with covariance analysis of $\log_e$ transformed, linearised disc size (DD)-increment data by site (data and fitted regression lines plotted in Fig. 7) with $\ln DD(t+1)$, where $t = 1$ yr, as response variable on the y-axis and $\ln DD(t)$ as the predictor variable on the x-axis and site as covariate (F is the variance ratio)

Grouped linear regression:

Source of variation	SS	df	MS	F	P
Common slope	10.360	1	10.36	2197.11	<0.0001
Common slope	10.360	1	10.36	2197.11	<0.0001
Between slopes	0.035	4	0.009	1.87	0.1198
Separate residuals	0.589	125	0.005		
Within groups	10.98	130			

Covariance analysis, uncorrected:

Source of variation	YY	xY	xX	df
Between groups	8.44	8.96	9.66	4
Within groups	10.98	12.77	15.75	130
Total	19.43	21.73	25.41	134

Corrected:

Source of variation	SS	df	MS	F
Between groups	0.217	4	0.054	11.22
Within groups	0.624	129	0.005	
Total	0.842	133		

Pairwise comparisons of sites:

	SRT	CRT	PSB3K	PSB4K	PAP
SRT		—	•	—	•
CRT	—			—	•
PSB3K	••	—			•
PSB4K	—	—	••		—
PAP	••	••	••	—	

• or •• denotes significant value of Student's t (df = 129) at $P<0.05$; • is for slope (upper half-matrix), •• is for slope separations, assuming a common slope (lower half-matrrix). $P<0.0001$.
SRT, SAMS Permanent Station in the southern Rockall Trough; CRT, Feni Ridge central Rockall Trough; PSB3K, ca. 3000 m Porcupine Seabight; PSB4K, ca. 4000 m Porcupine Seabight; PAP, *BENGAL* station Porcupine Abyssal Plain.

ossicle (Fig. 2) is implicit in the above growth analysis. This remains unproven for *O. hastatum*, just as it is to date from direct observations of growth of individuals of any deep-sea organisms. But a seasonal growth periodicity now appears very likely since the discovery of seasonally pulsed detrital flux to the seabed (Billett et al., 1983). This has been functionally linked to the discovery of annual reproductive cycles in some deep-sea benthic invertebrate species (Tyler et al., 1982; Campos-Creasey et al., 1994), and now from the present study in *O. hastatum*. Whether the assumed annual growth pattern in *O. hastatum* is in response to increased food or to metabolic diversion from somatic to reproductive growth consequent on reproductive seasonality is unknown. However, growth banding has already been found in the skeletal plates of a number of deep-sea ophiuroids and echinoids from the Rockall Trough, including species known both to reproduce seasonally (e.g. Gage, 1990b; Gage and Tyler, 1985), as well as those apparently reproducing year-round (Gage, 1990b; Gage, 1987). Growth banding was generally interpreted as reflecting zones of rapid skeletal growth possibly over a short period of time in spring/summer (in echinoderms reflected in zones of coarse-pored stereom). Each rapid-growth zone is followed by a band of slower, or possibly nil, growth probably encompassing a longer period in autumn/winter (bands of fine-pored stereom). As found in other brittle stars, the fine-pored bands in *O. hastatum* are also often associated with a radial ridge on the face of the vertebral fossa of the arm ossicles (Gage, 1990a, and see Figs 2B and C).

4.2. Differences in growth between sites

Comparison of growth at the five sites (Table 3) clearly shows that a common function adequately describes the data plotted in Fig. 7 even though the sites encompass a bathymetric range of about 2000 m to more than 4800 m depth. However, the pairwise comparisons of slope and line separations in Table 3 do suggest increasing difference in growth may occur with increasing depth separation of sites.

4.3. General interpretation of growth and reproduction in O. hastatum

The gametogenic pattern observed in *O. hastatum* from 4800 m at on the Porcupine Abyssal Plain is almost identical to the pattern of gametogenic development and seasonality seen in *Ophiura ljungmani* from 2900 m at the SAMS

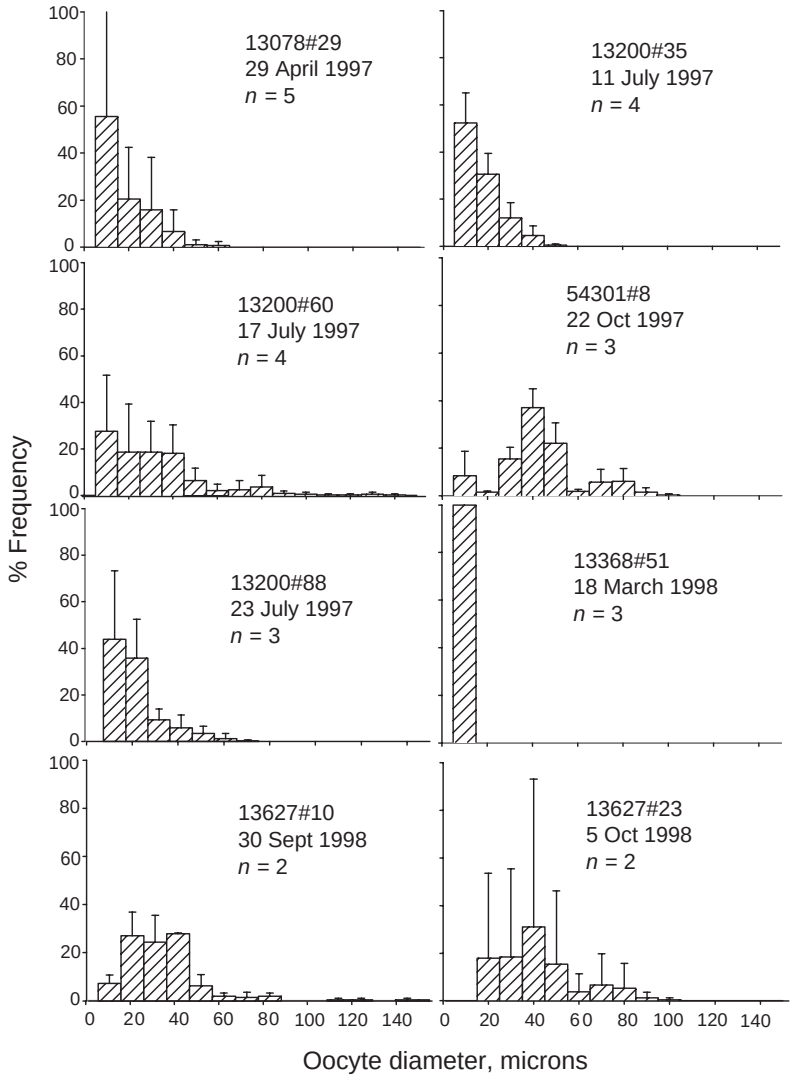

Fig. 8. Oocyte size/frequency data for samples of *O. hastatum* collected from the *BENGAL* Sta, Porcupine Abyssal Plain. Vertical boxes are mean oocyte diameter with whisker showing +1 *SD*; *n* is the number of individuals in the sample examined.

Permanent station in the southern Rockall Trough (Tyler and Gage, 1980). It is also very similar to that in *O. gracilis* from 900 m on the adjacent Hebridean continental margin (Sumida et al., 2000). Gametogenesis is initiated in late winter/early spring with oocyte growth accelerating after the arrival of the flux of phytodetritus to the deep-sea floor. Spawning would appear to take place in January/February of each year, a timing coincident with other species known to show seasonal gametogenic cycles in the deep NE Atlantic (Tyler et al., 1982; Tyler and Gage, 1984). The small egg size of *O. hastatum* is indicative of planktotrophic early development, although there is no candidate ophiopluteus larva known. Timing of settlement is also unknown, although by analogy with the congener *O. gracilis*, settlement of pelagic post-larvae is likely to occur in early summer.

Postlarval growth of the brittle star seems quite similar to the slightly sigmoidal, but overall rather linear, pattern seen in *O. gracilis* (fitted by a Gompertz growth function by Gage, 2003), and in

the upper abyssal ophiuroid *Ophiura ljungmani* (Gage and Tyler, 1982; Gage, 1990b). In other words growth in these three species does not appear to be particularly asymptotic. This contrasts to the pattern interpreted from growth bands in another deep-sea species *Ophiomusium lymani*. In the latter, size-at-age data from ossicle growth band measurements indicate relatively rapid growth of juveniles to a size where this heavily calcified epifaunal species achieves some protection from predation (Gage, 1990b). The contrasting growth strategy, as typified by *Ophiura ljungmani* by Tyler and Gage (1980), Gage and Tyler (1981) and Gage (1990b), is based on high reproductive fecundity and relatively low survivorship among both juveniles and adults. Reproductive maturity is reached at a quite small size with rather even growth increments because there is no particular advantage in achieving a large size as quickly as possible except in terms of increased fecundity. Growth in *Ophiura ljungmani* is expressed as a relatively low value of the growth constant (von Bertalanffy $K = 0.06$, Gompertz $K = 0.27$ from growth lines) and a growth asymptote, S_∞, may not be particularly obvious in pattern of growth banding. Estimate of the growth constant K are quite similar to this in the two deep-sea species of *Ophiocten,* (Gompertz $K = 0.27-0.28$ in *O. gracilis,* and $K = 0.20$ in *O. hastatum*; von Bertalanffy $K = 0.06-0.07$ in *O. gracilis,* and $K = 0.02$ in *O. hastatum,* all from pooled data).

4.4. Population abundance and size structure of *O. hastatum*

The considerably larger maximum size (17.7 mm disc diameter) recorded in our samples compared to the maximum previously known, 12 mm disc diameter (Paterson et al., 1982) may simply be a consequence of the rarity of *O. hastatum* in trawlings from the deep sea. We may add that the absence of any indication of a growth asymptote in the pattern of growth bands suggests potential to grow well beyond this size. The right-hand skewed mode in size structure (Fig. 5A) of the single exceptionally large sample (AT 121) from the SAMS Permanent Station in the southern Rockall Trough shows that a size $\geqslant 12$ mm disc diameter may not be unusual in this species. The relative rarity of *O. hastatum* is shown in other samples from this site. A maximum of 13 individuals (mean, 3.2) were taken in 25 hauls yielding *O. hastatum* taken from the area of the SAMS Permanent Station at 2900 m depth using various towed sampling devices from 1973 up to 1993 (J.D. Gage, unpublished data). Furthermore, *O. hastaum* was never collected from a total bottom area of 6 m^2 from 24 USNEL box corer samples (each sampling 0.25 m^2 and washed through a 0.42 mm sieve) taken at depths from 2000 to 2900 m depth on various dates from 1976 up to 1992 at various places in the Rockall Trough (J.D. Gage, unpublished data).

The total of 187 individuals in AT121 taken in 1976 from the SAMS Permanent Station was also unusually large compared with the maximum of two individuals from a total of five epibenthic sled hauls taken on other dates in 1976 from this site. Even if sled hauls collect fewer epifauna than the Agassiz trawl this large sample suggests strong patchiness in population abundance might occur.

The observed disc-size frequencies in AT121 with a strong right hand mode occurring between 13 and 17 mm disc diameter and lack of small sizes also presents an enigma. The peak in sizes was developed well beyond the mesh size range (10 mm) of the trawl net, and it was observed from other hauls included in the present study that in practice the Agassiz trawl is potentially able to catch individuals with disc diameters down to at least 5–8 mm in. This is probably because of increased retention of small sizes caused by the outstretched arms of the brittle star. We therefore conclude the apparent absence of smaller sizes in AT121 was real and not a sampling artifact.

The expectation for a species with a relatively low K and little evidence of the largest individuals approaching a growth asymptote (assuming moderate or high mortality) will be that numbers of larger sizes will decline with increasing age. This would give a left-skewed peak in size frequencies, or at least frequencies more evenly distributed along the size axis (Barry and Tegner, 1990; Gage, 1995). Because of this the peak is unlikely to represent a stack of older age classes approaching asymptotic size, as in *Ophiomusium lymani* (Gage and Tyler, 1982; Gage,

1990b, 1995). Rather, the absence of smaller sizes must result from lack of recruitment of more recent younger age classes to the population. The single mode suggests this was the result of above-usual recruitment of one or more year classes some years previously (see further discussion below).

This explanation fits with observations of temporal variability in abundance of *O. hastatum* from the Porcupine Abyssal Plain. Here trawlings and seabed photographs taken over the years 1989 up to 1999 at the *BENGAL* station indicated densities of brittle stars that include *O. hastatum* had increased from $<1\,m^{-2}$ to $>5\,m^{-2}$ (Bett et al., 2001). Results from twenty-five $0.25\,m^2$ boxes taken at this station on the Porcupine Abyssal Plain from 1996 to 1998 show a relatively high density, certainly compared to that generally prevailing at the SAMS Permanent Station in the southern Rockall Trough. The box cores yielded a total of six *O. hastatum* (personal communication, Joëlle Galéron and Myriam Sibuet, IFREMER, Brest) giving an estimated density of just under 1 *O. hastatum* m^{-2} (max. two individuals per core). Disc diameter measurements on these six specimens are included in Fig. 5B).

The apparent increase in brittle star abundance was accompanied by dramatic increase in population densities of megafaunal holothurians (*Amperima rosea* and *Ellipinion molle*) which showed a tenfold increase from the years 1989–1994 to 1997–1999 (Billett et al., 2001). The '*Amperima*' event has provided the first instance of major interannual change in megafaunal population densities in the NE Atlantic. That such variability may occur in the abyssal ocean has already been recorded from the abyssal eastern N Pacific where significant variation in abundances of benthic macro- and megafauna, and in sediment community oxygen consumption, over a 7-year time period has been recorded (Smith and Druffel, 1998; Smith and Kaufmann, 1999; Drazen et al., 1998; Lauerman and Kaufman, 1998). Long-term variability was previously unknown in the deep sea, probably because of the rarity of repeat sampling at fixed stations. Yet such variability remains unexpected because of supposedly stable environmental conditions thought until quite recently to prevail in this environment.

We assume that, like *O. gracilis,* individuals of *O. hastatum* will not be taken in coarse meshed trawls until they exceed about disc diameter ≈ 5–8 mm (assuming they retain their arms when collected by the gear). It follows that possibly one or more later year classes will not have been retained by the sampling gear. We postulate that the observed size frequencies (Fig. 3B), disc diameter range 5.9–7.6 mm, may represent the growth of one or more settlements in the years preceding 1996, possibly from 1993 to about 1995. Growth banding suggests a maximum age of 5 or 6 yr in two individuals taken in 1998 and 1997, respectively (7.6 and 6.9 mm disc diameter, respectively), with the remainder 3–4 yr.

Intriguingly the *Amperima* event coincided with the absence of phytodetrital mass deposition as observed from deployment of the time-lapse camera system Bathysnap in 1997–2000. This was in contrast to the years 1991–1994 when phytodetritus typically appeared as a blanketing layer on the sea floor from June to September with a seabed coverage of 50–96% in 1994 (Bett et al., 2001). Such mass deposition results from rapid transport to the deep ocean floor of detrital aggregates from primary production at the surface (Billett et al., 1983; Rice et al., 1994). Recently deposited phytodetritus was visible only as small aggregates on the surface of undisturbed multicorer samples taken from May to September in 1996–1999. Yet sediment traps set nearby in midwater fail to show any concomitant change in downward organic particle flux in the water column over this whole period (Lampitt et al., 2001). We note that the interpreted ages of *O. hastatum* from the *BENGAL* station indicate that all would have settled as post-larvae during the years when large amounts of phytodetrital mass deposition on the seabed seems to have occurred.

Gut contents analysis of *O. hastatum* suggest this species, in common with *Amperima* and *Ellipinion*, feeds nearly exclusively on fresh particulate organic matter (Iken et al., 2001). Bett et al. (2001) suggest from recording the movements of brittle stars in time lapse seabed photographs at the *BENGAL* station that the intensity of foraging of these numerically enhanced epibenthic populations prevented accumulation of phytodetritus on the seabed.

The usually low abundance of *O. hastatum* has to be considered against a reproductive strategy of small ripe egg size allowing relatively high fecundity and probable wide dispersal by pelagic larvae. With a preferred diet of newly settled detrital material, perhaps survivorship of settled post-larvae is improved when phytodetritus is readily available, although we cannot necessarily conclude that successful recruitment occurred because of this availability. If such phytodetrital deposition is locally patchy then an ensuing local population expansion of *O. hastatum* might explain the unusually large sample obtained by AT121 in the southern Rockall Trough where from personal observations of J.D.G. from multicorer samples phytodetrital mass deposition is also known to occur (see also observations cited in Beaulieu, 2002). Exceptionally large numbers of *O. hastatum* occurring very sporadically in samples has also been noted from French deep-sea sampling in the NE Atlantic (Dr Myriam Sibuet, IFREMER Brest, personal communication).

We believe that the reproductive strategy and growth characteristics of *O. hastatum* support an interpretation that this species, by its ability to exploit the somewhat ephemeral and patchy food resource provided by phytodetritus, is an opportunist. A similar conclusion was reached by Wigham et al. (2003) for the phytodetritus grazer *Amperima rosea* on the basis of early age of maturity, high fecundity and small egg size indicative of a planktotrophic or lecithotrophic early development resulting in potential for rapid population expansion during nutritional favourable conditions. We therefore suggest that substantial increases in population size of *O. hastatum* could occur locally, or over larger areas at the interannual time scale during similarly nutritionally favourable periods of mass deposition of phytodetritus.

Acknowledgements

We thank Robin Harvey at Dunstaffnage for assistance in the SEM examinations and photography and Brian Bett and David Billett of SOC, and Myriam Sibuet and Joëlle Galéron at IFREMER, Centre de Brest, France, for generously making available trawl and box-core material collected from the Porcupine Seabight and Porcupine Abyssal Plain, including that collected during the EU MAST III-funded *BENGAL* project, Contract No. MAS3-CT95-0018 (DG12—ESCY). We wish to thank the referees for their valuable suggestions for improving this paper and Dr Mike Burrows (SAMS) for statistical advice during preparation of a revised version.

References

Armitage, P., Berry, G., 1994. Statistical Methods in Medical Research 3rd Edition. Blackwell, Oxford.

Barry, J.P., Tegner, M.J., 1990. Inferring demographic processes from size-frequencey distributions: simple models indicate specific patterns of growth and mortality. Fishery Bulletin 88, 13–19.

Beaulieu, S.E., 2002. Accumulation and fate of phytodetritus on the sea floor. Oceanography and Marine Biology: an Annual Review 40, 171–232.

Bett, B.J., Malzone, M.G., Narayanaswamy, B.E., Wigham, B.D., 2001. Temporal activity in phytodetritus and megabenthic activity at the seabed in the deep Northeast Atlantic. Progress in Oceanography 50, 349–368.

Billett, D.S.M., Lampitt, R.S., Rice, A.L., Mantoura, R.F.C., 1983. Seasonal sedimentation of phytodetritus to the deep-sea benthos. Nature (London) 302, 520–522.

Billett, D.S.M., Bett, B.J., Rice, A.L., Thurston, M.H., Galeron, J., Sibuet, M., Wolff, G.A., 2001. Long-term changes in the megabenthos of the Porcupine Abyssal Plain (NE Atlantic). Progress in Oceanography 50, 325–348.

Brey, T., 2001. Population dynamics in benthic invertebrates. A Virtual Handbook, Version 01.2. http://www.awi-bremerhaven.de/Benthic/Ecosystem/FoodWeb/Handbook/main.html. Alfred Wegener Institute for Polar and Marine Research, Germany.

Brey, T., Pearse, J., Basch, L., McClintock, J., 1995. Growth and production of *Sterechinus neumayeri* (Echinoidea: Echinodermata) in McMurdo Sound, Antarctica. Marine Biology 124, 279–292.

Campos-Creasey, L.S., Tyler, P.A., Gage, J.D., John, A.W.G., 1994. Evidence for coupling the verticle flux iof phytodetritus to the diet and seasonal life history of the deep-sea echinoid *Echinus affinis*. Deep-Sea Research 41, 369–388.

Crisp, D.J., 1984. Energy flow measurement. In: Holme, N.A., McIntyre, A.D. (Eds.), Methods for the Study of Marine Benthos. IBP Handbook No. 16, 2nd Edition. Blackwell, Oxford, pp. 284–372.

Dahm, C., 1993. Growth, production and ecological significance of *Ophiura albida* and *O. ophiura* (Echinodermata: Ophiuroidea) in the German Bight. Marine Biology 116, 431–437.

Dahm, C., Brey, T., 1998. Determination of growth and age of slow-growing brittle stars (Echinodermata: Ophiuroidea) from natural growth bands. Journal of the Marine Biological Association of the United Kingdom 78, 941–951.

Drazen, J.C., Baldwin, R.J., Smith, K.L., 1998. Sediment community response to a temporally varying food supply to an abyssal station in the NE Pacific. Deep-Sea Research II 45, 893–913.

Ebert, T.A., Dixon, J.D., Shroeter, S.C., Kalvass, P.E., Richmond, N.T., Bradbury, W.A., Woodby, D.A., 1999. Growth and Mortality of red sea urchins *Strongylocentrotus franciscanus* across a latitudinal gradient. Marine Ecology Progress Series 190, 189–209.

Gage, J.D., 1987. Growth of the deep-sea irregular sea urchins *Echinosigra phiale* and *Hemiaster expergitus* in the Rockall Trough (N.E. Atlantic Ocean). Marine Biology 96, 19–30.

Gage, J.D., 1990a. Skeletal growth bands in brittle stars: microstructure and significance as age markers. Journal of the Marine Biological Association of the United Kingdom 70, 209–224.

Gage, J.D., 1990b. Skeletal growth markers in the deep–sea brittle stars *Ophiura 1jungmani* and *Ophiomusium lymani*. Marine Biology 104, 427–435.

Gage, J.D., 1995. Demographic modelling in the analysis of population dynamics of deep-sea macrobenthos. Internationale Revue der gesamten Hydrobiologie 80, 171–185.

Gage, J.D., 2003. Growth and production of *Ophiocten gracilis* (Ophiuroidea: Echinodermata) on the Scottish continental slope. Marine Biology 143, 85–97.

Gage, J.D., Tyler, P.A., 1981. Re-appraisal of age composition, growth and survivorship of the deep-sea brittle star *Ophiura ljungmani* from size structure in a sample time series from the Rockall Trough. Marine Biology 64, 163–172.

Gage, J.D., Tyler, P.A., 1982. Depth–related gradients in size structure and the bathymetric zonation of deep–sea brittle stars. Marine Biology 71, 299–308.

Gage, J.D., Tyler, P.A., 1985. Growth and recruitment of the deep-sea urchin *Echinus affinis*. Marine Biology 90, 41–53.

Gage, J.D., Pearson, M., Clark, A.M., Paterson, G.L.J., Tyler, P.A., 1983. Echinoderms of the Rockall trough and adjacent areas I. Crinoidea, Asteroidea and Ophiuroidea. Bulletins of the British Museum (Natural History), Zoology Series 45 (5), 263–308.

Harvey, R., Gage, J.D., Billett, D.S.M., Clark, A.M., Paterson, G.L.J., 1988. Echinoderms of the Rockall trough and adjacent areas 3. Additional records. Bulletins of the British Museum (Natural History), Zoology Series 54 (4), 153–198.

Iken, K., Brey, T., Wand, U., Voigt, J., Junghans, P., 2001. Food web structure of the benthic community at the Porcupine Abysal Plain (NE Atlantic): stable isotope analysis. Progress in Oceanography 50, 383–405.

Lampitt, R.S., Bett, B.J., Kiriakoulakis, K., Popova, E.E., Ragueneau, O., Vangriesheim, A., Wolff, G.A., 2001. Material supply to the abyssal seafloor in the Northeast Atlantic. Progress in Oceanography 50, 27–63.

Lauerman, L.M.L., Kaufman, R.S., 1998. Deep-sea epibenthic echinoderms and a temporally varying food supply: results from a one year time series in the NE Pacific. Deep-Sea Research II 45, 817–842.

Paterson, G.L.J., 1985. The deep-sea Ophiuroidea of the North Atlantic Ocean. Bulletin of the British Museum (Natural History), Zoology Series 49 (1), 1–162.

Paterson, G.L.J., Tyler, P.A., Gage, J.D., 1982. The taxonomy and zoogeography of the genus *Ophiocten* (Echinodermata: Ophiuroidea) in the North Atlantic Ocean. Bulletin of the British Museum (Natural History), Zoology Series 43 (3), 109–128.

Pearson, M., Gage, J.D., 1984. Diets of some deep-sea brittle stars in the Rockall Trough. Marine Biology 82, 247-258.

Rice, A.L., Thurston, M.H., Bett, B.J., 1994. The IOSDL DEEPSEAS programme: introduction and photographic evidence for the presene and absence of a seasonal input of; phytodetritus at contrasting sites in the northeastern Atlantic. Deep-Sea Research I 41, 1305–1320.

Schnute, J., 1981. A versatile growth model with statistically stable parameters. Canadian Journal of Fisheries and Aquatic Science 38, 1128–1140.

Smith, K.L., Druffel, E.R.M., 1998. Long time-series monitoring of an abyssal site in the NE Pacific: an introduction. Deep-Sea Research II 45, 573–586.

Smith, K.L., Kaufmann, R.S., 1999. Long-term discrepancy between food supply and demand in the deep eastern North Pacific. Science 284, 1174–1177.

Sumida, P.Y.G., Tyler, P.A., Lampitt, R.S., Gage, J.D., 2000. Reproduction, dispersal and settlement of the bathyal ophiuroid *Ophiocten gracilis* in the NE Atlantic Ocean. Marine Biology 137, 623–630.

Tanaka, M., 1982. A new growth curve which expresses infinite increase. Publications of the Amakusa Marine Biological Laboratory 9, 103–106.

Tyler, P.A., Gage, J.D., 1980. Reproduction and growth in the deep–sea brittle star *Ophiura ljungmani* (Lyman). Oceanologica Acta 3, 177–185.

Tyler, P.A., Gage, J.D., 1984. Seasonal reproduction of *Echinus affinis* (Echinodermata: Echinoidea) in the Rockall Trough, NE Atlantic. Deep-Sea Research 31, 387–402.

Tyler, P.A., Grant, A., Pain, S.L., Gage, J.D., 1982. Is annual reproduction in deep-sea echinoderms a response to variability in their environment? Nature (London) 300, 747–750.

Yamaguchi, M., 1975. Estimating growth parameters from growth rate data: problems with marine sedentary invertebrates. Oecologia Berlin 20, 321–332.

Wigham, B.D., Tyler, P.A., Billett, D.S.M., 2003. Reproductive biology of the abyssal holothurian *Amperima rosea*: an opportunistic response to variable flux of surface derived organic matter? Journal of the Marine Biological Association of the United Kingdom 83, 175–188.

Zar, J.H., 1998. Biostatistical Analysis 4th Edition. Prentice-Hall, New York.